Agricultural Sulfur Applications Alter the Quantity and Composition of Dissolved Organic Matter from Field-to-Watershed Scales

Anna L. Hermes,* Merritt N. Logan, Brett A. Poulin, Amy M. McKenna, Todd E. Dawson, Thomas Borch, and Eve-Lyn S. Hinckley*

Read Online

ACCESS | Metrics & More | Article Recommendations | Supporting Information

ABSTRACT: Over the past several decades, agricultural sulfur (S) use has dramatically increased. Excess S in the environment can cause several biogeochemical and ecologic consequences, including methylmercury production. This study investigated agriculturally associated changes to organic S—the most dominant form of S within soils—from field-to-watershed scales. Using a novel complementary suite of analytical methods, we combined Fourier transform ion cyclotron resonance mass spectrometry, δ^{34}S-DOS, and S X-ray absorption spectroscopy to characterize dissolved organic S (DOS) in soil porewater and surface water samples from vineyard agriculture (S addition) and forest/grassland areas (no S addition) within the Napa River watershed (California, U.S.). Vineyard soil porewater dissolved organic matter samples had two-fold higher S content compared to forest/grasslands and had unique $CHOS_2$ chemical formulas—the latter also found in tributary and Napa River surface water. The isotopic difference between δ^{34}S-DOS and δ^{34}S−SO_4^{2-} values provided insights into the likely dominant microbial S processes by land use/land cover (LULC), whereas the S oxidation state did not strongly differ by LULC. The results add to our understanding of the modern S cycle and point to upland agricultural areas as S sources with the potential for rapid S transformations in downgradient environments.
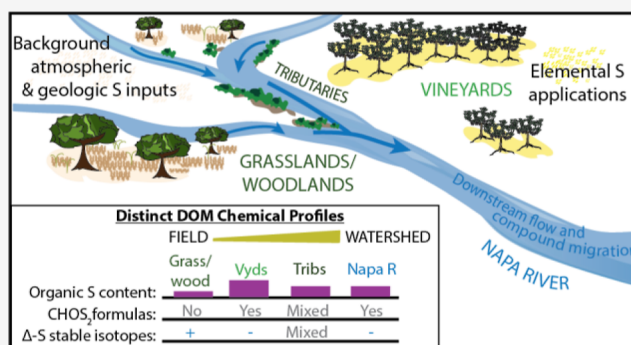
KEYWORDS: sulfur, stable isotopes, XANES, FT-ICR MS, land use, viticulture, mass spectrometry, dissolved organic matter

1. INTRODUCTION

Agricultural sulfur (S) applications are increasing worldwide in response to declines in atmospheric S deposition.[1,2] This change in human-driven alteration to the global S cycle mobilizes geologic, relatively non-reactive S into the biosphere. Compelling recent syntheses highlight the potential for excess S to cause significant ecosystem and human health consequences,[1,3] which gives new urgency to efforts aimed at determining the forms, amounts, and fates of agriculture-derived S species in the environment. As organic S is the most dominant form of S in both natural and agricultural soils,[4−7] investigating agricultural changes to the organic S pool is a critical step toward fully constraining the transport, transformations, and fates of agricultural S in the environment.

Organic S is intricately tied to elements of environmental concern, including mercury (Hg). Microbial sulfate reduction (MSR) stimulates methylmercury production, a neurotoxin that bio-accumulates in fish and wildlife.[8] Much of what we understand about the complex interactions between S and Hg stems from decades of research that linked agricultural S runoff to methylmercury production in Florida Everglades wetlands.[9,10] Researchers found that the speciation, atomic S content, and aromaticity of dissolved organic S (DOS) can act either to inhibit or stimulate methylmercury production. For example, sulfurization of dissolved organic matter (DOM) in Florida Everglades sediments has been linked to enhanced DOM reactivity,[11] as more aromatic DOS or DOS enriched in reduced S functionalities (e.g., thiolates) enhances methylmercury production.[12−14] These studies suggest that characterizing the molecular composition and speciation of DOS derived from agricultural areas is important for understanding agricultural S reactivity in the environment. However, there is a need to broaden investigations of DOS chemistry beyond wetland ecosystems, including upland agricultural areas or regional settings with mixed land use/land cover (LULC).

Within agricultural fields, DOS speciation and molecular composition may affect S storage within field soils versus mobilization to downgradient aquatic ecosystems, where it can interact with Hg and other biogeochemical cycles. Studies in
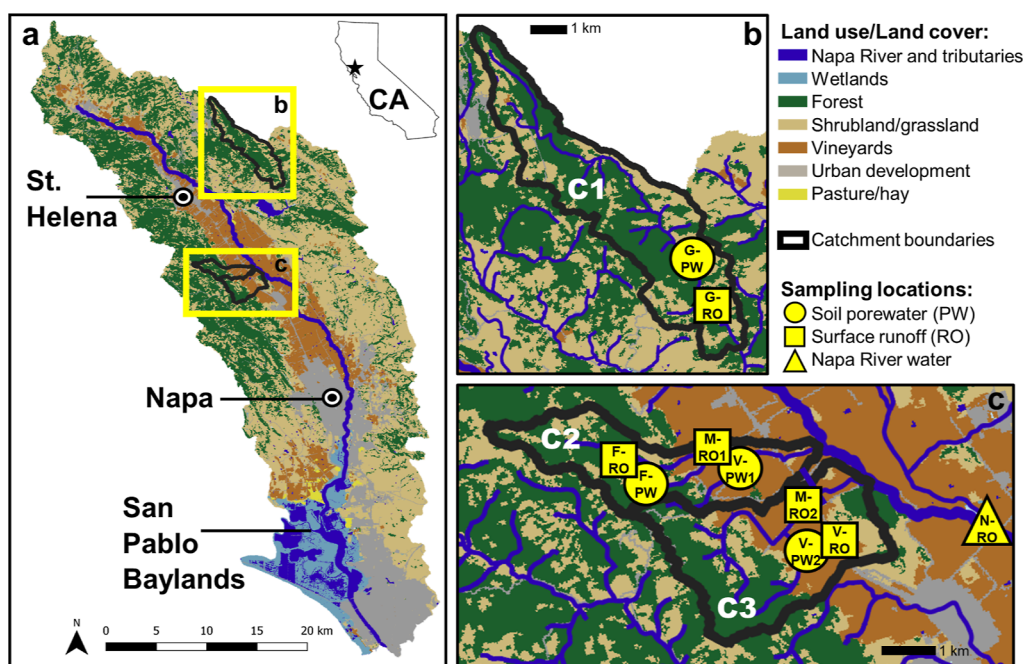
Figure 1. (a) Map and land use/land cover of the Napa River watershed, which drains into extensive wetlands in the San Pablo Baylands. Sample collection efforts were focused within three sub-catchments of the Napa River: (b) a forest/shrubland/grassland catchment (C1) and (c) two catchments with forested headwaters that then drain through vineyard agriculture (C2 and C3). G = grassland; F = forest; V = vineyard; M = mixed LULC; N = Napa River; PW = soil porewater; and RO = surface water runoff.

forested ecosystems that received high atmospheric S deposition demonstrated that adsorption of DOS to mineral soils lengthened the residence time of S within soils.[15,16] In terms of mobilization, agricultural areas export primarily low-molecular weight microbially-derived DOM with a higher proportion of S and nitrogen (N) heteroatoms.[17−19] Once in downstream aquatic ecosystems, DOS is subject to additional transformations. Recent studies with DOM and model compounds show that reduced DOS species are selectively photodegraded to inorganic sulfate (SO_4^{2-}),[20,21] a process that could enhance agricultural S transport. Finally, complex S cycling and hydrology in both agricultural and non-agricultural areas of a watershed may influence the degree to which agricultural S is mobilized and interacts with other elements downstream. Linking agricultural S applications to the composition of the organic S pool and the fate of agricultural S in broader ecosystems requires (1) analytical approaches that holistically characterize DOS chemistry and (2) an assessment of changes to DOS across spatial scales.

In this study, we employed multiple qualitative and quantitative analytical techniques to advance characterization of agricultural DOS in an upland, mixed LULC watershed. Given higher S inputs to agricultural areas compared to non-agricultural areas, we hypothesized that (1) the quantity of DOS is higher in agricultural areas compared to non-agricultural areas; (2) agricultural DOS is compositionally distinct from non-agricultural DOS; and (3) agricultural DOS is detectable in surface waters beyond fields. We used negative-ion electrospray ionization ultrahigh-resolution Fourier transform ion cyclotron resonance mass spectrometry (FT-ICR MS) at 21 tesla to qualitatively evaluate agricultural and non-agricultural molecular-level compound diversity[22] and to trace agricultural DOS beyond agricultural fields.[20] Sulfur K-edge X-ray absorption near-edge structure (XANES) spectroscopy quantified organic S speciation or the distribution of S

oxidation states.[23] Finally, we measured the ratio of S stable isotopes in organic matter (δ^{34}S-DOS), which has been used to differentiate DOS derived from assimilatory versus dissimilatory SO_4^{2-} reduction[24] and provides insight into S mineralization pathways.[25]

We build on prior research of agricultural S in the Napa River watershed,[7,26−29] where a $34 billion wine grape crop industry[30] requires intensive S applications averaging 80 kg S ha^{-1} yr^{-1} as S^0.[1] Vineyards are surrounded by forest and shrubland/grassland areas that receive atmospheric and geologic S sources, providing a natural contrast between areas of intensive S application and background S atmospheric deposition. To test our hypotheses, we analyzed soil porewater samples collected from vineyard and forest/shrubland/grassland (i.e., "non-agricultural") LULC areas (agricultural field scale, ∼0.15−2.5 ha) and sampled surface waters from mixed LULC tributaries and the Napa River (catchment-to-watershed-scales, ∼260−47,000 ha). Using our novel combination of advanced DOM characterization techniques, we "fingerprinted" agricultural DOS, providing a means to holistically investigate the link between agricultural S applications and changes to S chemistry.

2. MATERIALS AND METHODS

2.1. Site Description and Sample Collection. The Napa River flows into San Pablo Bay, connecting to extensive wetland ecosystems and the greater San Francisco Bay Estuary. The region's Mediterranean climate results in distinct wet and dry seasons. During the dry, growing season (∼May through September), vineyard fields are sprayed weekly to biweekly with S^0 to prevent powdery mildew disease. During the wet season (∼October through April), average precipitation ranges from 863 mm in St. Helena to 677 mm in Napa (1991−2020 annual precipitation normal)[31] and intermittent tributaries begin to flow.

Sampling campaigns were carried out during the 2019−2020 California wet season within the Napa River watershed (Figure 1; Table S1 and Figure S1 in the Supporting Information). We collected soil porewater and surface waters between 4 and 14 December 2019, which was during the first significant rainfall event of the season with 235 mm of precipitation (26 November to 13 December 2019) and a maximum of 12.7 m³ s⁻¹ streamflow in the Napa River (Supporting Information, Table S1 and Figure S1). We sampled surface waters again during low flow conditions 29 February to 1 March 2020 with 0.7 m³ s⁻¹ streamflow in the Napa River (Supporting Information, Table S1 and Figure S1). At the time of sampling, the 2020 water year was the driest year in a 20 year precipitation record,[32] totaling only 424 mm of precipitation in Napa.[33]

2.2. Sample Processing and Aqueous Chemical Analyses. A complete description of sample processing and analyses can be found in the Supporting Information. Briefly, we analyzed soil porewater and stream water samples for dissolved organic carbon (DOC), SO_4^{2-}, and total dissolved sulfur concentrations ([DOC], [SO_4^{2-}], and [TDS], respectively), DOM specific ultraviolet absorbance at 254 nm, $SUVA_{254}$, a proxy for DOM aromaticity,[34] and $\delta^{34}S-SO_4^{2-}$. Soil porewater samples were processed in an O_2-free glovebox to retain sample redox conditions prior to analyses.

We used solid-phase extraction for parallel DOM characterization using FT-ICR MS, S XANES spectroscopy, DOM carbon and S content ([C]-DOM and [S]-DOM, respectively), and $\delta^{34}S$-DOM analysis (see the Supporting Information). Salt-free DOM extracts were isolated from soil porewater and stream water samples using modified styrene divinyl benzene polymer resin (Bond Elut-PPL, Varian Inc., USA; modified following Dittmar et al.[35]). We chose to use the PPL sorbent because it has been widely used for FT-ICR MS analysis and performs generally well compared to other sorbents for S extraction.[36−38] We saved aliquots of PPL eluate for [DOC], UV−vis absorption, [SO_4^{2-}], and [TDS] analyses to check for sample breakthrough and calculate C recovery (see the Supporting Information). We report stable isotope values in conventional δ-notation in parts per thousand (‰), relative to the international standard Vienna-Canyon Diablo Troilite (VCDT). Analytical precision was ±0.4 for $\delta^{34}S-SO_4^{2-}$, ±0.2‰ for $\delta^{34}S$-DOM, and ±0.35% for [S]-DOM (Table S3).

2.3. FT-ICR MS Analysis. To identify compositional differences between vineyard agriculture and non-agricultural samples, we analyzed a sub-sample of the dried PPL-extracted DOM using FT-ICR MS (see the Supporting Information). Importantly, S species are lower in abundance and ionization efficiency than O_x compounds, and thus, identification benefited from improved sensitivity, high dynamic range, and ultrahigh mass resolving power only achievable with 21 tesla FT-ICR MS. Briefly, samples were re-suspended in 100% HPLC-grade methanol (target 200 ppm C)[39] and analyzed in negative-ion electrospray ionization mode (ESI−) with a custom-built hybrid linear ion trap FT-ICR MS equipped with a 21 T superconducting solenoid magnet[40,41] at the National High Magnetic Field Laboratory in Tallahassee, Florida. Time-domain transients of 3.1 s were conditionally co-added and acquired with the Predator data station that handled excitation and detection only, initiated by a TTL trigger from the commercial Thermo data station, with 100 time-domain acquisitions averaged for all experiments.[42] Mass spectra were phase-corrected following Xian et al.[43] and internally

calibrated with 10−15 highly abundant homologous series that span the entire molecular weight distribution (~150−200 individual calibrants) based on the "walking" calibration method.[44] Molecular formulae were assigned and post-processed using PetroOrg software.[45] One sample, V-PW1, had poor spectral quality (Figure S11) and was therefore excluded from further FT-ICR MS analyses. All 21 tesla FT-ICR MS mass spectrum files are publicly available via the Open Science Framework (https://osf.io/nh3zc/) at DOI: 10.17605/OSF.IO/NH3ZC.

Assigned formulas were summarized into elemental class distributions (normalized to relative intensity), the modified aromaticity index (AI_{mod}), nominal oxidation state of C (NOSC), and compound classes (see Supporting Information, Table S4). We calculated the percentage of S-containing heteroatom formulas and the formulaic S/C following Poulin et al.[46]

$$\% \, S - \text{containing formulas} = \frac{\sum \text{CHOS, CHNOS}}{\text{total formula count}} \times 100\%$$

$$\text{formulaic S/C} = \frac{\sum S_{at}}{\sum C_{at}}$$

where CHOS and CHNOS are the number of formulas containing S and N and S; S_{at} and C_{at} are the total number of S and C atoms, respectively, detected in a sample. Finally, we derived a "forest and grassland LULC endmember" by combining all S-containing heteroatom formulas from forest and grassland samples (F-PW, HF F-RO, LF F-RO, G-PW, and G-RO). We then compared the formulas in this general endmember to vineyard samples to determine unique vs shared S-containing heteroatoms across land use types.

2.4. Sulfur K-edge XANES Spectroscopy. We analyzed the PPL-extracted DOM by S K-edge XANES spectroscopy (beamline 4-3, Stanford Synchrotron Radiation Lightsource; complete details in the Supporting Information). The atomic fractions of S functionalities were determined by Gaussian curve fitting (GCF)[23] in the software program Athena.[47] Spectra were normalized using pre- (2450.0−2462.5 eV) and post-edge regions (2515.0−2527.5 eV). Precision and accuracy estimates, curve fitting parameters, GCF results, and the atomic fractions of S functionalities are detailed in the Supporting Information (Figures S18−S20 and Tables S8−S10). We report concentrations of S functionalities (reduced S, sulfoxide, sulfone, sulfonate, and organosulfate) relative to C, calculated by multiplying the fraction of each functionality by the measured atomic S/C.

2.5. Statistical Analyses. We analyzed all data using R statistical software (v. 4.0.4).[48] Concentrations and related chemical properties (e.g. atomic S/C-DOM) are reported as the median ± interquartile range. To test for differences in molecular composition across samples, we calculated Bray−Curtis dissimilarity matrices of normalized peak intensities[49,50] for all assigned DOM molecular formulae and CHOS + CHNOS formulae using the vegan package and "vegdist" function.[49−51] Dissimilarity values were hierarchically clustered into a dendrogram using the "hclust" function with a ward.D2 linkage method.[52] We combined multiple data analyses into a principal component analysis (PCA) to assess overall differences across samples (Figure S21).
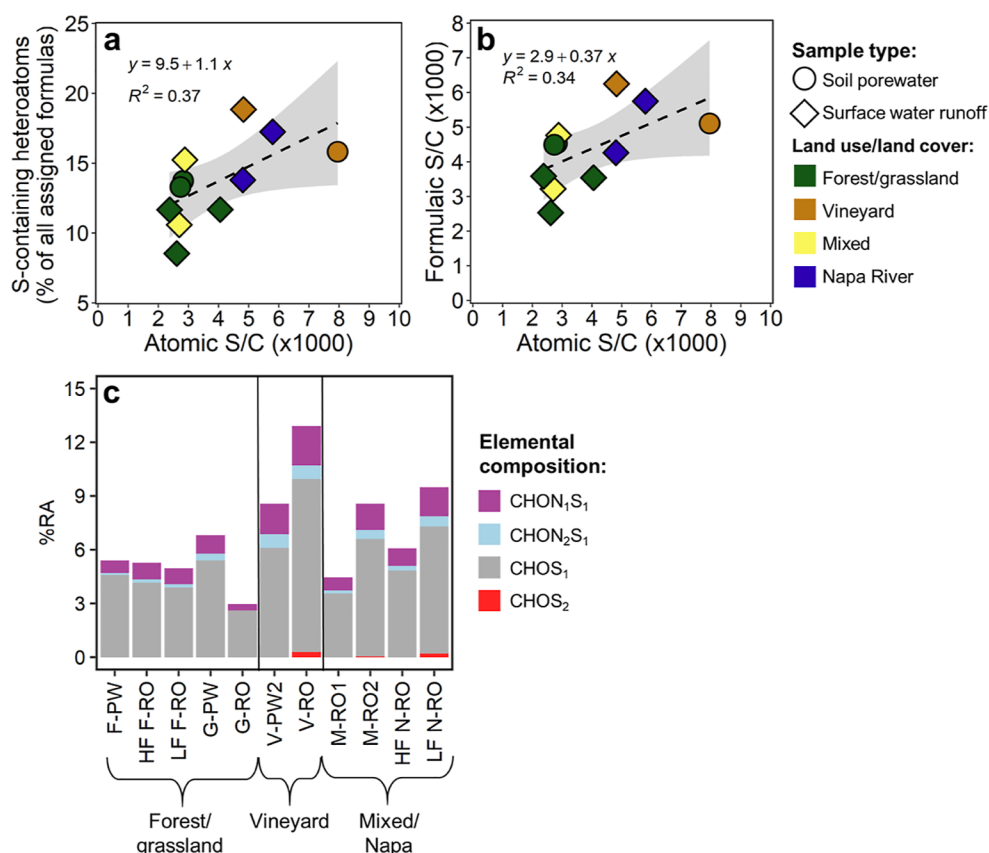
Figure 2. DOM sulfur content and molecular composition for different sample types and LULC. Linear correlations between the atomic S/C content of DOM and (a) S-containing heteroatoms as a percentage of total assigned formulas and (b) FT-ICR MS-derived formulaic S/C ratios show that vineyards have higher DOS content and S-containing formulas compared to forest and grassland samples. In (c), FT-ICR MS-derived S-containing formulas for each sample are normalized to sample RA. Sample abbreviations are as in Figure 1. HF = high streamflow; LF = low streamflow.

3. RESULTS

3.1. Sulfur and Carbon Concentrations. Comparing across LULC types, vineyard sample S concentrations were distinct from non-agricultural samples, but they did not show a trend in [DOC] or DOM SUVA$_{254}$. Vineyard samples had approximately four-fold higher SO$_4^{2-}$ concentrations relative to non-agricultural samples (14.5 ± 16.7 mg SO$_4^{2-}$−S L^{-1} vs 3.22 ± 3.81 mg SO$_4^{2-}$−S L^{-1}, respectively; Table S2). The highest SO$_4^{2-}$ concentration measured was in catchment 2: vineyard soil porewater (V-PW2), vineyard culvert runoff (V-RO), and mixed LULC stream runoff (M-RO2) had 14.5, 38.5, and 26.7 mg SO$_4^{2-}$−S L^{-1}, respectively. Like SO$_4^{2-}$, the influence of S inputs to vineyard areas was apparent in the atomic S/C of PPL-extracted DOM. Vineyard samples had approximately two-fold higher atomic S/C-DOM than non-agricultural samples, with median values of 4.83 × 10^{-3} and 2.73 × 10^{-3} mmol S mmol C^{-1}, respectively (Table S3). In contrast to S chemistry, DOC concentration did not differ by LULC type (Table S2) and neither did the DOM SUVA$_{254}$, which ranged from 1.36 L mg C^{-1} m^{-1} in grassland soil porewater (G-PW) to 3.74 L mg C^{-1} m^{-1} in grassland stream water runoff (G-RO; Table S2).

3.2. FT-ICR MS Characterization of DOS. FT-ICR MS results showed notable differences in S chemistry across LULC types. We observed a significant correlation between atomic S/C-DOM and the percent of S heteroatoms detected in FT-ICR MS spectra (Figure 2a) as well as the formulaic S/C (Figure

2b). The S heteroatom content was also strongly correlated with dissolved SO$_4^{2-}$ concentration (R^2 = 0.73; Figure S2). Vineyard samples (V-PW2 and V-RO) had 9 and 13% relative abundance (RA) of S-containing heteroatoms, whereas non-agricultural samples had only 3−7% RA of S-containing heteroatoms (Figure 2c). The increase in vineyard S-containing heteroatoms stemmed from an overall increase in the RA of all S-containing heteroatom classes (CHOS$_1$, CHON$_1$S$_1$, and CHON$_2$S$_1$; Figure 2c). Mixed LULC runoff M-RO1 and high flow Napa River runoff (HF N-RO) had S heteroatom distributions more similar to non-agricultural samples, while mixed LULC runoff M-RO2 and low flow Napa River runoff (LF N-RO) had higher proportions of CHOS$_1$ and CHON$_1$S$_1$ classes, similar to vineyard samples (Figure 2c). We detected low levels of CHOS$_2$ in three samples: vineyard culvert runoff, V-RO (0.27% total RA); mixed LULC stream runoff 2, M-RO2 (0.03% total RA); and the Napa River at low flow, LF N-RO (0.19% total RA; Figure 2c).

Given the higher S content and proportion of S-containing formula assignments in vineyard samples, we evaluated whether vineyard DOS was compositionally distinct from non-agricultural samples. The Bray−Curtis dissimilarity analysis clustered samples into two groups, which generally split into a "forest/grassland-dominated" group and a "vineyard-dominated" group (Figure 3a). The first group included the majority of non-agricultural samples (G-RO, LF F-RO, HF F-RO, and F-PW), as well as mixed stream runoff 1
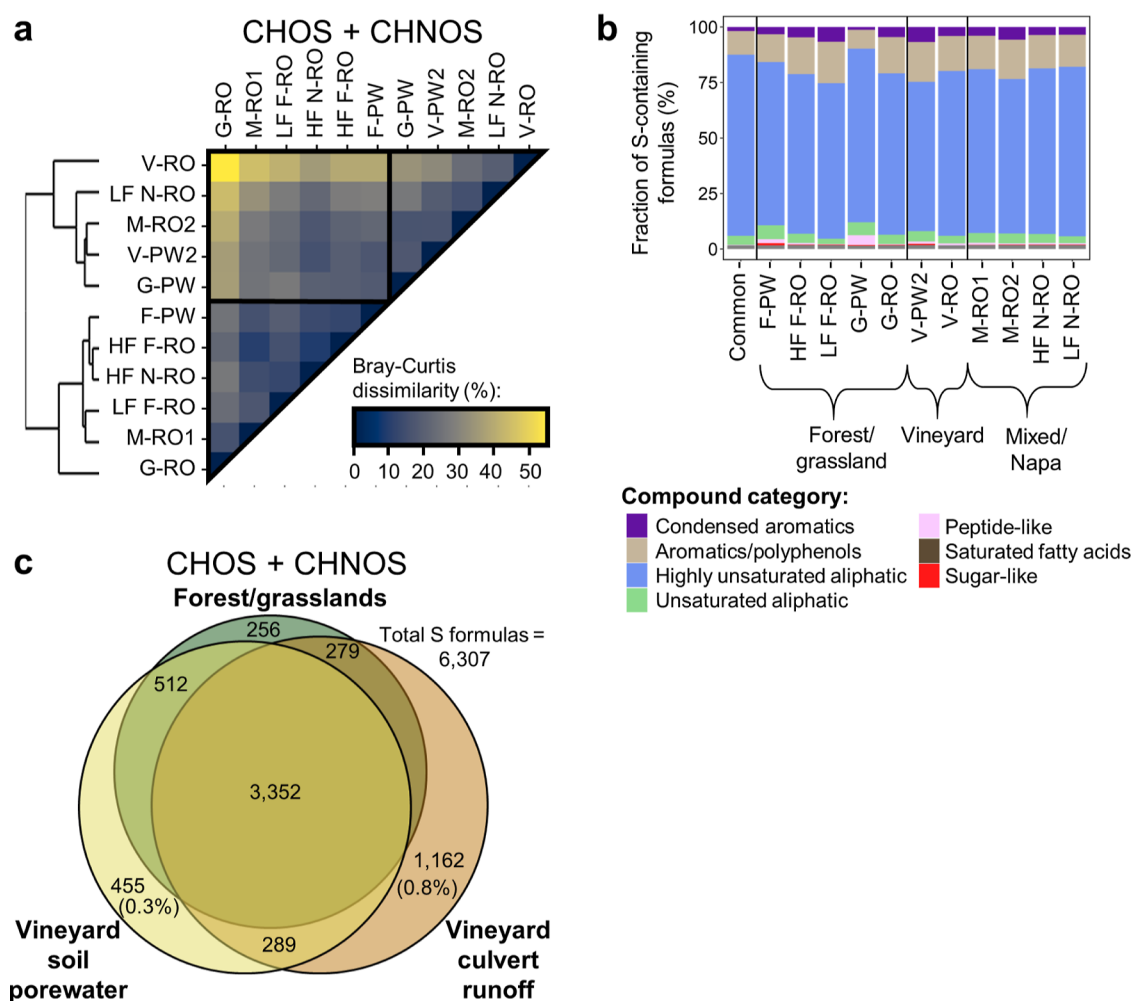
Figure 3. Compositional differences across samples. (a) Bray−Curtis dissimilarity matrix of intensity-weighted CHOS + CHNOS formulas showing that forest and grassland samples and vineyard samples generally cluster separately. Yellow represents higher dissimilarity, and blue represents lower dissimilarity. (b) van Krevelen-derived compound categories shown as percentages of total S-containing formulas. The "common" bar is the composition of CHOS + CHNOS formulas that are shared across all samples. (c) Venn diagram showing the number of unique and common CHOS + CHNOS formulas between V-PW2 (vineyard soil porewater), V-RO (vineyard culvert runoff), and a general forest/grassland LULC endmember, which includes F-PW, HF F-RO, LF F-RO, G-PW, and G-RO. Percentage values are the abundance of unique formulas relative to all assigned formulas.

(M-RO1), and the Napa River at high flow (HF N-RO). Samples within this group had 9−26% dissimilarity from one another. The second group included vineyard (V-PW2 and V-RO) as well as mixed stream runoff 2 (M-RO2), grassland (G-PW), and Napa River at low flow (LF N-RO) samples and exhibited dissimilarity values slightly higher than the first group from 15 to 33%. Across groups, the highest dissimilarity was between V-RO and G-RO at 55%, and the lowest dissimilarities were between the forest stream and Napa River at high flow (HF F-RO and HF N-RO) at 9% and between the forest stream at high flow and mixed stream runoff 1 (HF F-RO and M-RO1) at 10%. Soil porewater and culvert runoff samples from the vineyard (V-PW2 and V-RO, respectively) had relatively high dissimilarity at 31% despite coming from the same vineyard.

We further evaluated DOS composition across samples using van Krevelen putative compound categories (defined in Table S4). If Bray−Curtis dissimilarities were driven by differences in the number of formulas only, all samples would be expected to have similar distributions of formulas in van Krevelen space. We observed that highly unsaturated aliphatic

formulas dominated all samples at 69−78%, followed by either aromatic (1−12%) or unsaturated aliphatic formulas (8−17%; Figure 3b). However, several samples exhibited unique compound category distributions. For example, V-PW2 had the highest relative proportions of condensed (1.8%) and aromatic (11.8%) formulas compared to all other samples and a higher proportion of sugar-like formulas (0.7%) compared to most other samples. V-RO had minimal condensed formulas (<0.1%), a lower relative proportion of aromatic formulas (8.2%), and no sugar-like formulas. G-PW had the highest proportion of peptide-like (3.7%) and very low aromatic formulas (1.1%). Finally, F-PW was similar to G-PW, except for an increase in sugar-like formulas (1%). Mixed stream and Napa River samples had similar DOS compound category distributions.

We examined unique S-containing formulas (CHOS + CHNOS) to isolate drivers of the DOS compositional difference, comparing V-PW2, V-RO, and a general "forest/grassland" LULC endmember (Figure 3c). Roughly 50% of the DOS formulas were common to endmember samples, with 18% unique to vineyard culvert runoff (V-RO), 7% unique to
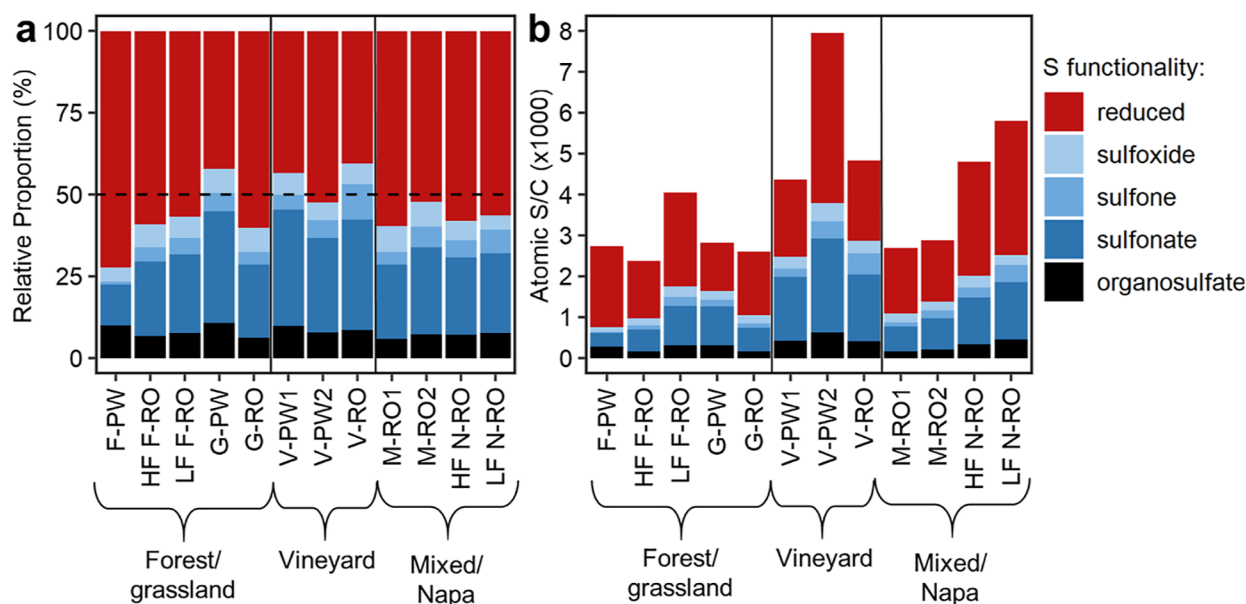
Figure 4. Sulfur K-edge XANES speciation results including the (a) relative proportions of reduced S (summation of exocyclic and heterocyclic reduced S), sulfoxide, sulfone, sulfonate, and organosulfate and (b) the ratio of sulfur functionalities relative to C in the DOM (as atomic S/C). The dashed line in subplot a represents equal proportions of reduced and oxidized-S species. Sample abbreviations are as in Figure 1.
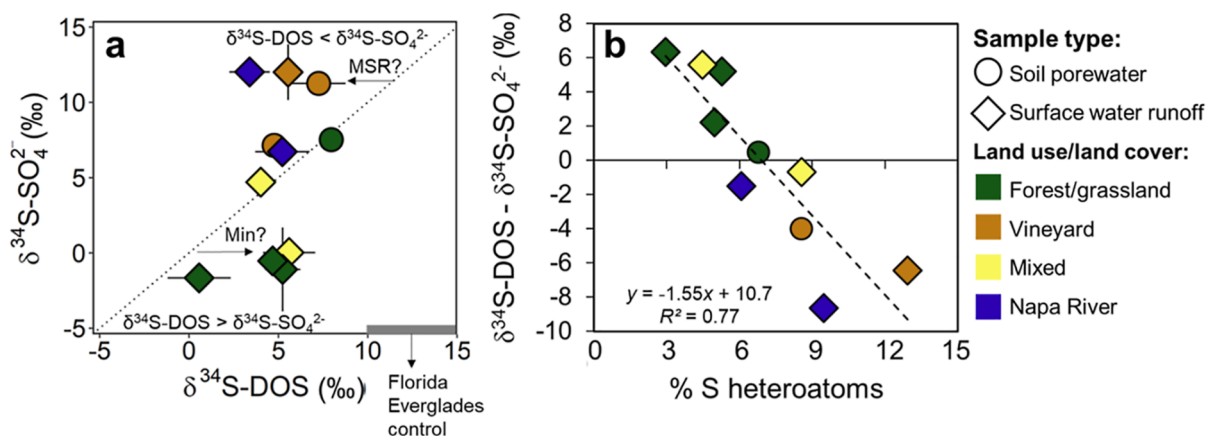

Figure 5. (a) Sulfur stable isotope values for inorganic sulfate ($\delta^{34}S-SO_4^{2-}$) and organic S ($\delta^{34}S$-DOS). Error bars show ± 1 SD. Dotted line is the 1:1 line of equal isotope values, and the gray bar shows the range of $\delta^{34}S$-DOS measured for control samples from the Florida Everglades (see the Supporting Information). (b) Relationship for the difference between organic and inorganic sulfur stable isotopes and the percent of S-containing heteroatom formulas as measured by FT-ICR MS.

vineyard soil porewater (V-PW2), and only 4% unique to all forest/grassland samples. S-containing formulas unique to vineyard culvert runoff (V-RO) were primarily $CHOS_1$ (31%), $CHON_1S_1$ (24%), and $CHOS_2$ (30%), with the remainder $CHON_2S_1$ (14%; Figure S3). S-containing formulas unique to vineyard soil pore water (V-PW2) were split equally among $CHOS_1$ (35%), $CHON_1S_1$ (33%), and $CHON_2S_1$ (31%). Conversely, S-containing formulas unique to non-agricultural sites were primarily $CHOS_1$ (75%), with smaller contributions from $CHON_1S_1$ (21%) and $CHON_2S_1$ (4%).

The vast majority of mixed stream and Napa River S-containing formulas were shared with LULC endmembers or other mixed LULC samples. Remarkably, M-RO1 and HF N-RO samples shared 98.7 and 99.3% of S-containing formulas with another sample, respectively, the majority of which were shared with one or more LULC endmembers (F-PW, HF F-RO, FL F-RO, G-PW, G-RO, V-PW2, and V-RO; Figure S4). M-RO2 shared 95.9% of its S-containing formulas with another

sample, and all of its 54 $CHOS_2$ formulas were shared with V-RO (Figure S5). The LF N-RO sample had the lowest proportion of shared formulas at 88.3% (Figure S4), but the majority of its $CHOS_2$ formulas were also present in the V-RO spectrum (Figure S5).

3.3. DOS Oxidation State. Sulfur XANES results showed variable proportions of organic S oxidation states in soil porewaters and streams (Figure 4). Relative proportions of S functionalities did not differ systematically by LULC or soil/ stream sample type. Instead, forest and grassland samples ranged from 42% reduced S (exocyclic + heterocyclic) in G-PW to 72% in F-PW, the highest reduced S proportion observed as primarily exocyclic reduced S (Table S8). Vineyard samples had either roughly equal proportions of reduced and oxidized species (48%, V-PW2) or higher oxidized S at 56−60% (V-PW1 and V-RO, respectively). Mixed LULC streams and the Napa River had 52−60% reduced S, similar to HF and LF F-RO, G-RO, and V-PW2.

For all samples, sulfonate was the primary form of oxidized S functionalities. When normalized to atomic S/C, vineyard soil porewater, V-PW2, had the highest reduced S content at 4.2×10^{-3} mmol S mmol C^{-1} (Figure 4b).

3.4. Sulfur Stable Isotope Ratios. Sulfur stable isotope ratios were distinct between vineyard and non-agricultural samples, largely driven by differences in $\delta^{34}S-SO_4^{2-}$ values rather than $\delta^{34}S$-DOS values. Inorganic $\delta^{34}S-SO_4^{2-}$ values ranged from −1.7 to 12‰ (Figure 5a), and vineyard samples were enriched in ^{34}S by ~12‰ (11.3 ± 2.4‰) compared to forest and grassland samples (−0.81 ± 2.7‰). Mixed stream runoff 1 (M-RO1) fell within the forest and grassland range of $\delta^{34}S-SO_4^{2-}$ values at 0.025‰, whereas M-RO2 was more similar to vineyard values at 4.7‰. Napa River samples were within the vineyard $\delta^{34}S-SO_4^{2-}$ at high and low flows, 6.7 and 12.0‰, respectively. Organic S stable isotope values ranged from 0.56 to 8.0‰, spanning a smaller range in $\delta^{34}S$ ratios than inorganic $\delta^{34}SO_4^{2-}$ values (Figure 5b). $\delta^{34}S$-DOS values did not appear to differ by LULC but did differ in relation to $\delta^{34}S-SO_4^{2-}$ values. Non-agricultural $\delta^{34}S$-DOS values were 0.44–6.2‰ enriched relative $\delta^{34}S-SO_4^{2-}$ values, whereas vineyard $\delta^{34}S$-DOS values were 2.4–6.5‰ depleted relative to $\delta^{34}S-SO_4^{2-}$ values. The difference between $\delta^{34}S$-DOS and $\delta^{34}S-SO_4^{2-}$ was negatively correlated with the % S heteroatoms of the DOM ($R^2 = 0.77$). Multivariate PCA analysis reinforced separation in DOS chemistry between vineyard and non-agricultural LULC types (Supporting Information, Figure S21).

4. DISCUSSION

4.1. Agricultural S Additions Increase DOS Content. Agricultural S applications increased the S content of DOM relative to surrounding non-agricultural areas, supporting our first hypothesis. Increased DOS content was apparent in bulk [S]-DOM measurements (Table S3), the FT-ICR MS-derived formulaic S/C and S-containing formula abundances (Figure 2), as well as the strong correlation between SO_4^{2-} concentration and the abundance of S-containing heteroatoms in DOM (Figure S2). The general agreement between bulk measurements and FT-ICR MS results suggests that FT-ICR MS can be used semi-quantitatively to assess DOS content, as previously observed in the Florida Everglades by Poulin et al.[46] Our measurements of vineyard atomic S/C ($4.4–8.0 \times 10^{-3}$ mmol S mmol C^{-1}) were in between those from agriculturally non-impacted and impacted surface waters of the Florida Everglades (~$4–5 \times 10^{-3}$ mmol S mmol C^{-1} and ~$7.5–8.5 \times 10^{-3}$ mmol S mmol C^{-1}, respectively), a highly reducing environment where S is abiotically incorporated into DOM.[46] Higher S-heteroatom content in vineyard samples is also consistent with prior studies that have shown agricultural areas have higher heteroatom content in DOM compared to forested ecosystems.[17,19,53]

4.2. Agricultural Versus Forest and Grassland DOS Sources and Transformations. Dissolved organic S molecular composition and speciation provided insights into DOS sources and transformations in agricultural and non-agricultural soils and streams. Although organic S molecular composition did differ between agricultural and non-agricultural samples, there was also significant formula overlap (Figure 3c), implicating shared S sources and transformations across land use types. This suggests that our second hypothesis—that agricultural DOS is compositionally distinct from non-agricultural DOS—is partially validated. For

example, soil porewater samples from both vineyard agriculture and non-agricultural areas likely reflect microbial S cycling during the early-season sampling campaign, which is supported by high proportions of unsaturated aliphatic, peptide-like, and sugar-like DOM formulas (Figure 3b) and lower DOM $SUVA_{254}$ (Table S2) compared to stream water samples.[17,54,55] One vineyard (V-PW1) and grassland soil porewater (G-PW) had a higher proportion of oxidized than reduced S (Figure 4a), also consistent with a microbial-derived DOS source.[56] Our findings that microbial OM predominated in soil porewaters from both vineyard and non-agricultural areas differ from prior studies showing that cropland streams typically have higher microbial-derived DOM than forests.[19,57,58] In contrast to soil porewater samples, non-agricultural streams (G-RO, HF F-RO, LF F-RO, and M-RO1) strongly reflect flushing of fresh, plant-derived OM stored in soils,[17,19] with lower overall heteroatom content (Table S5), higher $SUVA_{254}$ values, higher AI_{mod}, and higher average formula mass (Figure 5b, Table S2, and Table S7).

Sulfur stable isotope patterns further elucidated differences in DOS transformations across LULC types. Enriched $\delta^{34}S$-DOS values of forest and grassland stream water relative to $\delta^{34}S-SO_4^{2-}$ are consistent with measurements in the Black Forest, Germany and spruce forests in the Czech Republic and has been attributed to plant-OM S mineralization, which leads to a slight enrichment in ^{34}S-DOS relative to SO_4^{2-}.[59,60] Samples that had nearly equivalent $\delta^{34}S$-DOS and $\delta^{34}S-SO_4^{2-}$ values (Figure 5a) could either reflect DOS produced via pathways with minimal fractionation or mixing of agricultural and non-agricultural S sources. Since FT-ICR MS and S XANES results suggest that soil porewater DOS reflected a microbial source, similar $\delta^{34}S$-DOS and $\delta^{34}S-SO_4^{2-}$ values in F-PW and V-PW1 could be further evidence of assimilatory SO_4^{2-} reduction since this process results in minimal S fractionation (~1−3‰).[24,61] Mixing of sources is a more likely explanation for mixed LULC stream runoff (M-RO2) and the Napa River at high flow (HF N-RO), since stream samples had higher DOM $SUVA_{254}$ and molecular evidence pointed to a flushing of fresh DOS (Table S2).

Vineyard and Napa River samples with $\delta^{34}S$-DOS values lower than $\delta^{34}S-SO_4^{2-}$ could either represent simply a difference in organic and inorganic S sources or could be an indicator for SO_4^{2-} reduction followed by DOM sulfurization. Evidence for abiotic incorporation of reduced S species into DOM has grown in recent years across a range of ecosystems including prairie potholes,[62] the Florida Everglades,[46] groundwater in the Adirondack Mountains, New York,[24] mangrove roots,[63] Antarctic lakes,[64] and oceans.[50,65] In most studies, sulfurization is tied to anaerobic sulfidic conditions, but SO_4^{2-} reduction and subsequent DOM sulfurization could also occur in soil anoxic microsites during periods of intermittent-to-sustained soil saturation.[66−68] We invoke the latter mechanism here because of the strong correlation between the difference in $\delta^{34}S$-DOS and $\delta^{34}S-SO_4^{2-}$ values and S heteroatom content, with $\delta^{34}S$-DOS < $\delta^{34}S-SO_4^{2-}$ values having a higher percentage of S-containing formulas (Figure 5). Conversely, if differences in the DOS source were responsible for this pattern, we would have expected S heteroatom content to be uniform across $\delta^{34}S$-DOS and $\delta^{34}S-SO_4^{2-}$ values which was not the case. Notably, however, the proposed sulfurization of OM within vineyards is not as extensive as measured in more reduced ecosystems (e.g., sulfidic wetlands and lakes).[62,64]

4.3. Sub-catchment-to-Watershed Scale DOS Chemistry. Mixed LULC stream and Napa River organic S chemistry provided insights into the traceability of the agricultural S fingerprint through the Napa River watershed. Streams that receive a combination of inputs from different land covers had DOS chemistry that reflected the predominant land cover. For example, the M-RO1 catchment area is 91.6% non-agricultural land cover (Table S1), and M-RO1 DOS chemistry was more similar to non-agricultural samples (F-PW, HF F-RO, and G-RO) than vineyard samples (Figures 3a and S21). In contrast, the M-RO2 catchment is 23.2% vineyard agriculture LULC (Table S1) and DOS had low dissimilarity values and similar S speciation compared to vineyard soil porewater (Figure 3a and Figure 4). Vineyard-derived DOS in M-RO2 was reinforced by the presence, albeit low abundance, of $CHOS_2$ formulas in the vineyard culvert runoff (V-RO; Figure 2c, Figure S4, Figure S5, and Table S5), detection of which was enabled by the very high mass resolution of the FT-ICR MS analysis. These results suggest that vineyard-derived DOS is transported beyond fields, is traceable, and influences the DOS chemistry of receiving stream waters, supporting our third hypothesis.

At the watershed scale, Napa River samples showed a shift in DOS composition between high and low flow conditions. At high flow (HF N-RO), the DOS chemistry shared characteristics with non-agricultural DOS, with a lower abundance of S-containing heteroatoms (Figure 2c) and depleted $\delta^{34}S-SO_4^{2-}$ values (Figure 5a). At low flow (LF N-RO), the DOS chemistry was strongly influenced by vineyard DOS, with a higher proportion of S-containing heteroatoms (Figure 2c), enriched $\delta^{34}S-SO_4^{2-}$ values (Figure 5a), and the presence of vineyard-derived $CHOS_2$ formulas (Figure 3c, Figure S4, and Figure S5). Several studies have attributed enhanced $CHOS_1$ content in rivers to wastewater inputs.[69] Although there are a number of relatively small wastewater treatment plants within the Napa River watershed, Napa River FT-ICR MS spectra did not have surfactant-like low-molecular weight peaks (typical for domestic wastewater) and had an average m/z of ~516, higher than the average of 314 m/z measured from wastewater effluents[69] (Table S7, Figure S16, and Figure S17). These results suggest that Napa River DOS is more likely reflecting the vineyard S source. Combining multiple analyses strengthened our ability to differentiate the vineyard DOS fingerprint in this complex and dynamic watershed.

Importantly, only 1 and 12% of Napa River assigned formulas were unique at high and low flow, respectively (Figure S4), suggesting that our endmember sampling captured much of the watershed's molecular diversity. The Napa River results indicate that non-agricultural DOS dominates at watershed scales during high flow, while vineyard-derived DOS dominates at low flows. One explanation for the change in source contributions across flow conditions is that vineyard hydrology is intensively controlled through growing season irrigation and subsurface drainage, potentially extending the duration of vineyard hydrologic transport longer than in the surrounding ecosystems. Nonetheless, our samples represent snapshots of the watershed's hydrology, and future studies are crucial to directly link daily-to-seasonal hydrologic dynamics and DOS composition and transport.

4.4. Implications for the Fate of Agricultural Sulfur. When mobilized beyond agricultural fields, DOS remains reactive and is subject to additional transformations such as photodegradation in surface waters. For example, in a laboratory experiment, Ossola et al.[20] found that 10−50% of DOS was mineralized to SO_4^{2-} after irradiation exposure equivalent to one midsummer day and was enhanced with high DOS content and microbial-derived OM—akin to the DOS found in vineyard culvert runoff (V-RO). The selective photooxidation of reduced DOS to SO_4^{2-} was confirmed by S XANES.[21] These findings suggest that mobilized vineyard DOS likely undergoes photodegradation, which could increase SO_4^{2-} concentrations and S mobility. However, if photodegradation significantly altered DOS along flow paths, we might expect that Napa River DOS would have a substantially different molecular composition than source areas. Instead, we found a high degree of formula commonality (Figure S4), suggesting that photodegradation and other S transformations do not strongly alter DOS chemistry at the spatial scale and under the flow conditions of this study.

Our characterization of both agricultural and non-agricultural DOS has implications for the ultimate fate and reactivity of agricultural S applications, especially related to trace elements of Hg and arsenic (As). Mercury methylation is often tied to microbial SO_4^{2-} reduction in wetlands and is enhanced in the presence of aromatic DOM with higher reduced S content.[14,70] Our measurements show that both non-agricultural and vineyard areas mobilize DOM with these characteristics (Figure 3b and Figure 4b), and vineyard samples had high concentrations of SO_4^{2-} (Table S2). Hence, SO_4^{2-} and DOS mobilized from different LULC areas of a watershed may intersect along flow paths and within wetlands to affect Hg methylation processes or downstream DOM alterations in receiving wetlands. Furthermore, As sequestration and release from soils in wetlands is intimately linked to organic S speciation and S cycling.[71] Our results inform where process-based studies are needed to better understand the environmental fate of agricultural S. For example, the influence of agricultural S on Hg methylation processes is understudied in the redox gradients associated with stream hyporheic and riparian zones.[72,73] Furthermore, the presence of high Hg methylation rates in the San Pablo Baylands[74−76]—just downgradient of the Napa River watershed—suggests that regional-scale studies are necessary to evaluate the interactions of agricultural S runoff and Hg.

The combined use of $\delta^{34}S$-DOS, S XANES, and FT-ICR MS analyses permitted an atomic- and molecular-level investigation of DOS sources and transformations and identified an agricultural DOS fingerprint in a watershed with complex and dynamic S biogeochemistry. The sampling design enabled the connection between S source applications and DOS chemistry at catchment and watershed scales for the first time, providing an approach to trace this human perturbation to the global S cycle and to enable studies to determine the consequences of excess S in adjacent ecosystems. Together, the findings emphasize that the reactivity of agricultural S and consequences for diverse biogeochemical processes are intricately tied to the chemistry of surrounding LULC types. Ultimately, this study reinforces the need to investigate interactions between agricultural S and elemental flows from surrounding ecosystems and across scales.

■ ASSOCIATED CONTENT

Ⓢ Supporting Information

The Supporting Information is available free of charge at https://pubs.acs.org/doi/10.1021/acs.est.3c01347.

Sample locations, dates, and collection, chemical analyses, DOM isolation details, FT-ICR MS analysis details, FT-ICR MS results, FT-ICR MS spectra and van Krevelen diagrams, sulfur K-edge XANES spectroscopy details, PPL recovery, δ^{34}S-DOM stable isotope validation, δ^{34}S results, and principal component analysis (PDF)

■ AUTHOR INFORMATION

Corresponding Authors

Anna L. Hermes − *Department of Environmental Studies, University of Colorado Boulder, Boulder, Colorado 80303, United States; Institute of Arctic and Alpine Research, University of Colorado Boulder, Boulder, Colorado 80303, United States;* Present Address: Water Quality Department, Northern Colorado Water Conservancy District, Berthoud, CO, 80513, United States; orcid.org/0000-0001-6499-1657; Email: ahermes@northernwater.org

Eve-Lyn S. Hinckley − *Department of Environmental Studies, University of Colorado Boulder, Boulder, Colorado 80303, United States; Institute of Arctic and Alpine Research, University of Colorado Boulder, Boulder, Colorado 80303, United States;* Present Address: Cooperative Institute for Research in Environmental Sciences, UCB 216, Boulder, CO 80309; Department of Ecology and Evolutionary Biology, University of Colorado - Boulder, Boulder, CO 80309; Email: eve.hinckley@colorado.edu

Authors

Merritt N. Logan − *Department of Chemistry, Colorado State University, Fort Collins, Colorado 80523, United States*

Brett A. Poulin − *Department of Environmental Toxicology, University of California Davis, Davis, California 95616, United States;* orcid.org/0000-0002-5555-7733

Amy M. McKenna − *National High Magnetic Field Laboratory, Florida State University, Tallahassee, Florida 32310, United States; Department of Soil and Crop Sciences, Colorado State University, Fort Collins, Colorado 80523, United States;* orcid.org/0000-0001-7213-521X

Todd E. Dawson − *Department of Integrative Biology, Department of Environmental Science, Policy & Management, and Center for Stable Isotope Biogeochemistry, University of California Berkeley, Berkeley, California 94720, United States*

Thomas Borch − *Department of Chemistry, Colorado State University, Fort Collins, Colorado 80523, United States; Department of Soil and Crop Sciences, Colorado State University, Fort Collins, Colorado 80523, United States;* orcid.org/0000-0002-4251-1613

Complete contact information is available at:
https://pubs.acs.org/10.1021/acs.est.3c01347

Notes

The authors declare no competing financial interest.

The scripts used to produce figures and analyze data are provided on GitHub (https://github.com/annahermes). All FT-ICR mass spectral data are publicly available through the Open Science Framework at DOI: 10.17605/OSF.IO/NH3ZC/.

■ REFERENCES

(1) Hinckley, E. L. S.; Crawford, J. T.; Fakhraei, H.; Driscoll, C. T. A Shift in Sulfur-Cycle Manipulation from Atmospheric Emissions to Agricultural Additions. *Nat. Geosci.* **2020**, *13*, 597−604.

(2) Feinberg, A.; Stenke, A.; Peter, T.; Hinckley, E.-L. S.; Driscoll, C. T.; Winkel, L. H. E. Reductions in the Deposition of Sulfur and Selenium to Agricultural Soils Pose Risk of Future Nutrient Deficiencies. *Commun. Earth Environ.* **2021**, *2*, 101.

(3) Zak, D.; Hupfer, M.; Cabezas, A.; Jurasinski, G.; Audet, J.; Kleeberg, A.; McInnes, R.; Kristiansen, S. M.; Petersen, R. J.; Liu, H.; Goldhammer, T. Sulphate in Freshwater Ecosystems: A Review of Sources, Biogeochemical Cycles, Ecotoxicological Effects and Bioremediation. *Earth-Sci. Rev.* **2021**, *212*, 103446.

(4) Tabatabai, M. A. Importance of Sulphur in Crop Production. *Biogeochemistry* **1984**, *1*, 45−62.

(5) Germida, J. J.; Janzen, H. H. Factors Affecting the Oxidation of Elemental Sulfur in Soils. *Fertil. Res.* **1993**, *35*, 101−114.

(6) Likens, G. E.; Driscoll, C. T.; Buso, D. C.; Mitchell, M. J.; Lovett, G. M.; Bailey, S. W.; Siccama, T. G.; Reiners, W. A.; Alewell, C. The Biogeochemistry of Sulfur at Hubbard Brook. *Biogeochemistry* **2002**, *60*, 235−316.

(7) Hinckley, E.-L. S.; Fendorf, S.; Matson, P. Short-Term Fates of High Sulfur Inputs in Northern California Vineyard Soils. *Nutr. Cycling Agroecosyst.* **2011**, *89*, 135−142.

(8) Gilmour, C. C.; Henry, E. A.; Mitchell, R. Sulfate Stimulation of Mercury Methylation in Freshwater Sediments. *Environ. Sci. Technol.* **1992**, *26*, 2281−2287.

(9) Bates, A. L.; Orem, W. H.; Harvey, J. W.; Spiker, E. C. Tracing Sources of Sulfur in the Florida Everglades. *J. Environ. Qual.* **2002**, *31*, 287−299.

(10) Orem, W.; Gilmour, C.; Axelrad, D.; Krabbenhoft, D.; Scheidt, D.; Kalla, P.; McCormick, P.; Gabriel, M.; Aiken, G. Sulfur in the South Florida Ecosystem: Distribution, Sources, Biogeochemistry, Impacts, and Management for Restoration. *Crit. Rev. Environ. Sci. Technol.* **2011**, *41*, 249−288.

(11) Poulin, B.; Gerbig, C. A.; Kim, C. S.; Stegemeier, J. P.; Ryan, J. N.; Aiken, G. R. Effects of Sulfide Concentration and Dissolved Organic Matter Characteristics on the Structure of Nanocolloidal Metacinnabar. *Environ. Sci. Technol.* **2017**, *51*, 13133−13142.

(12) Graham, A. M.; Aiken, G. R.; Gilmour, C. C. Effect of Dissolved Organic Matter Source and Character on Microbial Hg

Methylation in Hg−S−DOM Solutions. *Environ. Sci. Technol.* **2013**, *47*, 5746−5754.

(13) Manceau, A.; Lemouchi, C.; Enescu, M.; Gaillot, A.-C.; Lanson, M.; Magnin, V.; Glatzel, P.; Poulin, B. A.; Ryan, J. N.; Aiken, G. R.; Gautier-Luneau, I.; Nagy, K. L. Formation of Mercury Sulfide from Hg(II)−Thiolate Complexes in Natural Organic Matter. *Environ. Sci. Technol.* **2015**, *49*, 9787−9796.

(14) Graham, A. M.; Cameron-Burr, K. T.; Hajic, H. A.; Lee, C.; Msekela, D.; Gilmour, C. C. Sulfurization of Dissolved Organic Matter Increases Hg−Sulfide−Dissolved Organic Matter Bioavailability to a Hg-Methylating Bacterium. *Environ. Sci. Technol.* **2017**, *51*, 9080−9088.

(15) Mitchell, M. J.; Driscoll, C. T.; Fuller, R. D.; David, M. B.; Likens, G. E. Effect of Whole-Tree Harvesting on the Sulfur Dynamics of a Forest Soil. *Soil Sci. Soc. Am. J.* **1989**, *53*, 933−940.

(16) Mitchell, M. J.; Lovett, G.; Bailey, S.; Beall, F.; Burns, D.; Buso, D.; Clair, T. A.; Courchesne, F.; Duchesne, L.; Eimers, C.; Fernandez, I.; Houle, D.; Jeffries, D. S.; Likens, G. E.; Moran, M. D.; Rogers, C.; Schwede, D.; Shanley, J.; Weathers, K. C.; Vet, R. Comparisons of Watershed Sulfur Budgets in Southeast Canada and Northeast US: New Approaches and Implications. *Biogeochemistry* **2011**, *103*, 181−207.

(17) Wagner, S.; Riedel, T.; Niggemann, J.; Vähätalo, A. V.; Dittmar, T.; Jaffé, R. Linking the Molecular Signature of Heteroatomic Dissolved Organic Matter to Watershed Characteristics in World Rivers. *Environ. Sci. Technol.* **2015**, *49*, 13798−13806.

(18) Seifert, A. G.; Roth, V. N.; Dittmar, T.; Gleixner, G.; Breuer, L.; Houska, T.; Marxsen, J. Comparing Molecular Composition of Dissolved Organic Matter in Soil and Stream Water: Influence of Land Use and Chemical Characteristics. *Sci. Total Environ.* **2016**, *571*, 142−152.

(19) Spencer, R. G. M.; Kellerman, A. M.; Podgorski, D. C.; Macedo, M. N.; Jankowski, K.; Nunes, D.; Neill, C. Identifying the Molecular Signatures of Agricultural Expansion in Amazonian Headwater Streams. *J. Geophys. Res.: Biogeosci.* **2019**, *124*, 1637−1650.

(20) Ossola, R.; Tolu, J.; Clerc, B.; Erickson, P. R.; Winkel, L. H. E.; McNeill, K. Photochemical Production of Sulfate and Methanesulfonic Acid from Dissolved Organic Sulfur. *Environ. Sci. Technol.* **2019**, *53*, 13191−13200.

(21) Poulin, B. A. Selective Photochemical Oxidation of Reduced Dissolved Organic Sulfur to Inorganic Sulfate. *Environ. Sci. Technol. Lett.* **2023**, *10*, 499−505.

(22) Bahureksa, W.; Tfaily, M. M.; Boiteau, R. M.; Young, R. B.; Logan, M. N.; McKenna, A. M.; Borch, T. Soil Organic Matter Characterization by Fourier Transform Ion Cyclotron Resonance Mass Spectrometry (FTICR MS): A Critical Review of Sample Preparation, Analysis, and Data Interpretation. *Environ. Sci. Technol.* **2021**, *55*, 9637−9656.

(23) Manceau, A.; Nagy, K. L. Quantitative Analysis of Sulfur Functional Groups in Natural Organic Matter by XANES Spectroscopy. *Geochim. Cosmochim. Acta* **2012**, *99*, 206−223.

(24) Kang, P. G.; Mitchell, M. J.; Mayer, B.; Campbell, J. L. Isotopic Evidence for Determining the Sources of Dissolved Organic Sulfur in a Forested Catchment. *Environ. Sci. Technol.* **2014**, *48*, 11259−11267.

(25) Fuller, R. D.; Mitchell, M. J.; Krouse, H. R.; Wyskowski, B. J.; Driscoll, C. T. Stable Sulfur Isotope Ratios as a Tool for Interpreting Ecosystem Sulfur Dynamics. *Water, Air, Soil Pollut.* **1986**, *28*, 163−171.

(26) Hinckley, E.-L. S.; Kendall, C.; Loague, K. Not All Water Becomes Wine: Sulfur Inputs as an Opportune Tracer of Hydrochemical Losses from Vineyards. *Water Resour. Res.* **2008**, *44*, 1−14.

(27) Hinckley, E.-L. S.; Matson, P. A. Transformations, Transport, and Potential Unintended Consequences of High Sulfur Inputs to Napa Valley Vineyards. *Proc. Natl. Acad. Sci. U.S.A.* **2011**, *108*, 14005−14010.

(28) Hermes, A. L.; Ebel, B. A.; Murphy, S. F.; Hinckley, E.-L. S. Fates and Fingerprints of Sulfur and Carbon Following Wildfire in Economically Important Croplands of California, U.S. *Sci. Total Environ.* **2021**, *750*, 142179.

(29) Hermes, A. L.; Dawson, T. E.; Hinckley, E.-L. S. Sulfur Isotopes Reveal Agricultural Changes to the Modern Sulfur Cycle. *Environ. Res. Lett.* **2022**, *17*, 054032.

(30) Napa Valley Vintners. Napa valley fast facts https://napavintners.com/press/docs/napa_valley_fast_facts.pdf (accessed June 24, 2022).

(31) Arguez, A.; Durre, I.; Applequist, S.; Vose, R. S.; Squires, M. F.; Yin, X.; Heim, R. R.; Owen, T. W. NOAA's 1981−2010 U.S. Climate Normals: An Overview. *Bull. Am. Meteorol. Soc.* **2012**, *93*, 1687−1697.

(32) Blank, P. October Rainfall Report. *Napa County Resource Conservation District Monthly Newsletter*, November 2021.

(33) Napa County. Napa County Onerain. https://napa.onerain.com/ (accessed May 19, 2023).

(34) Weishaar, J. L.; Aiken, G. R.; Bergamaschi, B. A.; Fram, M. S.; Fujii, R.; Mopper, K. Evaluation of Specific Ultraviolet Absorbance as an Indicator of the Chemical Composition and Reactivity of Dissolved Organic Carbon. *Environ. Sci. Technol.* **2003**, *37*, 4702−4708.

(35) Dittmar, T.; Koch, B.; Hertkorn, N.; Kattner, G. A Simple and Efficient Method for the Solid-Phase Extraction of Dissolved Organic Matter (SPE-DOM) from Seawater. *Limnol. Oceanogr.: Methods* **2008**, *6*, 230−235.

(36) Pohlabeln, A. M.; Dittmar, T. Novel Insights into the Molecular Structure of Non-Volatile Marine Dissolved Organic Sulfur. *Mar. Chem.* **2015**, *168*, 86−94.

(37) Li, Y.; Harir, M.; Uhl, J.; Kanawati, B.; Lucio, M.; Smirnov, K. S.; Koch, B. P.; Schmitt-Kopplin, P.; Hertkorn, N. How Representative Are Dissolved Organic Matter (DOM) Extracts? A Comprehensive Study of Sorbent Selectivity for DOM Isolation. *Water Res.* **2017**, *116*, 316−323.

(38) Stücheli, P. E.; Niggemann, J.; Schubert, C. J. Comparison of Different Solid Phase Extraction Sorbents for the Qualitative Assessment of Dissolved Organic Nitrogen in Freshwater Samples Using FT-ICR-MS. *J. Limnol.* **2018**, *77*, 400−411.

(39) Cao, D.; Rao, Z.; Geng, F.; Niu, H.; Shi, Y.; Cai, Y.; Kang, Y. Advanced Molecular-Fingerprinting Analysis of Dissolved Organic Sulfur by Electrospray Ionization-Fourier Transform Ion Cyclotron Resonance Mass Spectrometry Using Optimal Spray Solvent. *J. Environ. Sci.* **2020**, *97*, 67−74.

(40) Hendrickson, C. L.; Quinn, J. P.; Kaiser, N. K.; Smith, D. F.; Blakney, G. T.; Chen, T.; Marshall, A. G.; Weisbrod, C. R.; Beu, S. C. 21 Tesla Fourier Transform Ion Cyclotron Resonance Mass Spectrometer: A National Resource for Ultrahigh Resolution Mass Analysis. *J. Am. Soc. Mass Spectrom.* **2015**, *26*, 1626−1632.

(41) Smith, D. F.; Podgorski, D. C.; Rodgers, R. P.; Blakney, G. T.; Hendrickson, C. L. 21 Tesla FT-ICR Mass Spectrometer for Ultrahigh-Resolution Analysis of Complex Organic Mixtures. *Anal. Chem.* **2018**, *90*, 2041−2047.

(42) Blakney, G. T.; Hendrickson, C. L.; Marshall, A. G. Predator Data Station: A Fast Data Acquisition System for Advanced FT-ICR MS Experiments. *Int. J. Mass Spectrom.* **2011**, *306*, 246−252.

(43) Xian, F.; Hendrickson, C. L.; Blakney, G. T.; Beu, S. C.; Marshall, A. G. Automated Broadband Phase Correction of Fourier Transform Ion Cyclotron Resonance Mass Spectra. *Anal. Chem.* **2010**, *82*, 8807−8812.

(44) Savory, J. J.; Kaiser, N. K.; Mckenna, A. M.; Xian, F.; Blakney, G. T.; Rodgers, R. P.; Hendrickson, C. L.; Marshall, A. G. Parts-Per-Billion Fourier Transform Ion Cyclotron Resonance Mass Measurement Accuracy with a "Walking" Calibration Equation. *Anal. Chem.* **2011**, *83*, 1732−1736.

(45) Corilo, Y. E. PetroOrg Software; The Florida Station University: Tallahassee, FL, 2012.

(46) Poulin, B. A.; Ryan, J. N.; Nagy, K. L.; Stubbins, A.; Dittmar, T.; Orem, W.; Krabbenhoft, D. P.; Aiken, G. R. Spatial Dependence of Reduced Sulfur in Everglades Dissolved Organic Matter Controlled by Sulfate Enrichment. *Environ. Sci. Technol.* **2017**, *51*, 3630−3639.

(47) Ravel, B.; Newville, M. ATHENA,ARTEMIS,HEPHAESTUS: data analysis for X-ray absorption spectroscopy usingIFEFFIT. *J. Synchrotron Radiat.* **2005**, *12*, 537−541.

(48) R Core Team. R. *A Language and Environment for Statistical Computing*; R Foundation For Statistical Computing: Vienna, 2021.

(49) Seidel, M.; Manecki, M.; Herlemann, D. P. R.; Deutsch, B.; Schulz-Bull, D.; Jürgens, K.; Dittmar, T. Composition and Transformation of Dissolved Organic Matter in the Baltic Sea. *Front. Earth Sci.* **2017**, *5*, 31.

(50) Gomez-Saez, G. V.; Dittmar, T.; Holtappels, M.; Pohlabeln, A. M.; Lichtschlag, A.; Schnetger, B.; Boetius, A.; Niggemann, J. Sulfurization of Dissolved Organic Matter in the Anoxic Water Column of the Black Sea. *Sci. Adv.* **2021**, *7*, No. eabf6199.

(51) Oksanen, J.; Guillaume Blanchet, F.; Friendly, M.; Kindt, R.; Legendre, P.; McGlinn, D.; Minchin, P. R.; O'Hara, R. B.; Simpson, G. L.; Solymos, P.; Stevens, M. H. H.; Szoecs, E.; Wagner, H. *Vegan: Community Ecology Package*, 2020.

(52) Murtagh, F.; Legendre, P. Ward's Hierarchical Agglomerative Clustering Method: Which Algorithms Implement Ward's Criterion? *J. Classif.* **2014**, *31*, 274−295.

(53) Roebuck, J. A.; Seidel, M.; Dittmar, T.; Jaffe, R. Controls of Land Use and the River Continuum Concept on Dissolved Organic Matter Composition in an Anthropogenically Disturbed Subtropical Watershed. *Environ. Sci. Technol.* **2020**, *54*, 195−206.

(54) Brooker, M. R.; Longnecker, K.; Kujawinski, E. B.; Evert, M. H.; Mouser, P. J. Discrete Organic Phosphorus Signatures Are Evident in Pollutant Sources within a Lake Erie Tributary. *Environ. Sci. Technol.* **2018**, *52*, 6771−6779.

(55) Kellerman, A. M.; Guillemette, F.; Podgorski, D. C.; Aiken, G. R.; Butler, K. D.; Spencer, R. G. M. Unifying Concepts Linking Dissolved Organic Matter Composition to Persistence in Aquatic Ecosystems. *Environ. Sci. Technol.* **2018**, *52*, 2538−2548.

(56) Edwards, P. J. *Sulfur Cycling, Retention, and Mobility in Soils: A Review*; U.S. Department of Agriculture, Forest Service, Northeastern Research Station, 1998.

(57) Wilson, H. F.; Xenopoulos, M. A. Effects of Agricultural Land Use on the Composition of Fluvial Dissolved Organic Matter. *Nat. Geosci.* **2009**, *2*, 37−41.

(58) Chen, S.; Du, Y. X.; Das, P.; Lamore, A. F.; Dimova, N. T.; Elliott, M.; Broadbent, E. N.; Roebuck, J. A.; Jaffé, R.; Lu, Y. H. Agricultural Land Use Changes Stream Dissolved Organic Matter via Altering Soil Inputs to Streams. *Sci. Total Environ.* **2021**, *796*, 148968.

(59) Mayer, B.; Fritz, P.; Prietzel, J.; Krouse, H. R. The Use of Stable Sulfur and Oxygen Isotope Ratios for Interpreting the Mobility of Sulfate in Aerobic Forest Soils. *Appl. Geochem.* **1995**, *10*, 161−173.

(60) Novák, M.; Kirchner, J. W.; Fottová, D.; Prechová, E.; Jǎcková, I.; Krám, P.; Hruska, J. Isotopic Evidence for Processes of Sulfur Retention/Release in 13 Forested Catchments Spanning a Strong Pollution Gradient (Czech Republic, Central Europe). *Global Biogeochem. Cycles* **2005**, *19*, 4012.

(61) Kaplan, I. R.; Rittenberg, S. C. Microbiological Fractionation of Sulphur Isotopes. *Microbiology* **1964**, *34*, 195−212.

(62) Sleighter, R. L.; Chin, Y.-P.; Arnold, W. A.; Hatcher, P. G.; McCabe, A. J.; McAdams, B. C.; Wallace, G. C. Evidence of Incorporation of Abiotic S and N into Prairie Wetland Dissolved Organic Matter. *Environ. Sci. Technol. Lett.* **2014**, *1*, 345−350.

(63) Raven, M. R.; Fike, D. A.; Gomes, M. L.; Webb, S. M. Chemical and Isotopic Evidence for Organic Matter Sulfurization in Redox Gradients Around Mangrove Roots. *Front. Earth Sci.* **2019**, *7*, 98.

(64) Aiken, G.; Mcknight, D.; Harnish, R.; Wershaw, R. Geochemistry of Aquatic Humic Substances in the Lake Fryxell Basin, Antarctica. *Biogeochemistry* **1996**, *34*, 157−188.

(65) Abdulla, H. A.; Burdige, D. J.; Komada, T. Abiotic Formation of Dissolved Organic Sulfur in Anoxic Sediments of Santa Barbara Basin. *Org. Geochem.* **2020**, *139*, 103879.

(66) Hansel, C. M.; Fendorf, S.; Jardine, P. M.; Francis, C. A. Changes in Bacterial and Archaeal Community Structure and Functional Diversity along a Geochemically Variable Soil Profile. *Appl. Environ. Microbiol.* **2008**, *74*, 1620−1633.

(67) Barton, L. L.; Fauque, G. D. Chapter 2 Biochemistry, Physiology and Biotechnology of Sulfate-Reducing Bacteria. In *Advances in Applied Microbiology*; Laskin, A. I., Sariaslani, S., Gadd, G. M., Eds.; Elsevier Inc., 2009; Vol. 68, pp 41−98.

(68) Santana, M. M.; Dias, T.; Gonzalez, J. M.; Cruz, C. Transformation of Organic and Inorganic Sulfur− Adding Perspectives to New Players in Soil and Rhizosphere. *Soil Biol. Biochem.* **2021**, *160*, 108306.

(69) Gonsior, M.; Zwartjes, M.; Cooper, W. J.; Song, W.; Ishida, K. P.; Tseng, L. Y.; Jeung, M. K.; Rosso, D.; Hertkorn, N.; Schmitt-Kopplin, P. Molecular Characterization of Effluent Organic Matter Identified by Ultrahigh Resolution Mass Spectrometry. *Water Res.* **2011**, *45*, 2943−2953.

(70) Graham, A. M.; Aiken, G. R.; Gilmour, C. C. Dissolved Organic Matter Enhances Microbial Mercury Methylation under Sulfidic Conditions. *Environ. Sci. Technol.* **2012**, *46*, 2715−2723.

(71) Langner, P.; Mikutta, C.; Kretzschmar, R. Arsenic Sequestration by Organic Sulfur in Peat. *Nat. Geosci.* **2011**, *5*, 66−73.

(72) Creswell, J. E.; Kerr, S. C.; Meyer, M. H.; Babiarz, C. L.; Shafer, M. M.; Armstrong, D. E.; Roden, E. E. Factors Controlling Temporal and Spatial Distribution of Total Mercury and Methylmercury in Hyporheic Sediments of the Allequash Creek Wetland, Northern Wisconsin. *J. Geophys. Res.: Biogeosci.* **2008**, *113*, G00C02. DOI: 10.1029/2008jg000742.

(73) Poulin, B. A.; Aiken, G. R.; Nagy, K. L.; Manceau, A.; Krabbenhoft, D. P.; Ryan, J. N. Mercury Transformation and Release Differs with Depth and Time in a Contaminated Riparian Soil during Simulated Flooding. *Geochim. Cosmochim. Acta* **2016**, *176*, 118−138.

(74) Marvin-DiPasquale, M. C.; Agee, J. L.; Bouse, R. M.; Jaffe, B. E. Microbial Cycling of Mercury in Contaminated Pelagic and Wetland Sediments of San Pablo Bay, California. *Environ. Geol.* **2003**, *43*, 260−267.

(75) Marvin-DiPasquale, M.; Windham-Myers, L.; Agee, J. L.; Kakouros, E.; Kieu, L. H.; Fleck, J. A.; Alpers, C. N.; Stricker, C. A. Methylmercury Production in Sediment from Agricultural and Non-Agricultural Wetlands in the Yolo Bypass, California, USA. *Sci. Total Environ.* **2014**, *484*, 288−299.

(76) Robinson, A.; Richey, A.; Slotton, D.; Collins, J.; Davis, J. North Bay Mercury Biosentinel Project, 2018.